A robust fuzzy clustering algorithm using spatial information combined with local membership filtering for brain MR images

Lanting Li
College of Computer Science and Engineering, Key Laboratory of Intelligent Computing in Medical Image Northeastern University
Shenyang, China
1910637@stu.neu.edu.cn

Peng Cao*
College of Computer Science and Engineering, Key Laboratory of Intelligent Computing in Medical Image, Ministry of Education Northeastern University
Shenyang, China
caopeng@cse.neu.edu.cn

Jinzhu Yang
College of Computer Science and Engineering Northeastern University
Shenyang, China
yangjinzhu@cse.neu.edu.cn

Dazhe Zhao
College of Computer Science and Engineering Northeastern University
Shenyang, China
zhaodz@neusoft.com

Osmar R. Zaiane
Alberta Machine Intelligence Institute University of Alberta
Edmonton, Canada
zaiane@ualberta.ca

Abstract—MRI brain segmentation plays an important part in computer-aided diagnosis, which visually reveals the changes in brain structure for doctors to quickly and accurately discover and treat diseases related to brain tissue morphology. The fuzzy c-means (FCM) algorithm performs well when the segmenting images with no noise and with intensity uniformity. However, the MRI brain images are always defective in noise and intensity non-uniformity and thus we propose a novel FCM algorithm named adaptive FCM with neighborhood membership (FCM_anm). We design a filtering process with neighborhood membership to reduce the negative influence of noise and a novel objective function which further considers the spatial membership information adaptively. Finally, to verify the performance of our method, several experiments comparing among the Experimental results demonstrate the proposed method consistently outperforms the state-of-the-art FCM-based algorithms in synthetic images, simulated and real brain MR images with effects of the noise and intensity non-uniformity.

Index Terms—MRI brain segmentation, Fuzzy c-means algorithm, Spatial information, Local membership filtering, Adaptive penalty item

I. INTRODUCTION

Researching on brain tissue segmentation in neuroimaging is essential to study any brain related disorders and structural changes accompanied by changes in gray matter (GM), white matter (WM) or cerebrospinal fluid (CSF) sizes, such as schizophrenia, dementia and multiple sclerosis [1] [2]. Magnetic resonance imaging (MRI) is usually the modality of choice for structural brain analysis, since it provides images with high soft-tissue contrasts and high spatial resolution. MRI is most often used for the diagnosis and detection of tumors, lesions, to observe tissues growth, treatment planning and other abnormalities in brain soft tissues. Manual segmentation is extremely time-consuming due to millions of voxels in the brain MRI image. Besides, the segmentation result is prone to substantial intra-observer and inter-observer variation. Therefore, it is essential to propose an effective approach for computer-aided diagnosis of brain tissues from the MRI image.

Various methods have been proposed by researchers on MRI brain tissue segmentation including atlas-based segmentation methods [3] [4] [5], supervised machine learning methods and fuzzy clustering methods [3] [6] [7] [8]. Several segmentation methods for brain MR imaging have been reported in the literature in the recent past [9]. Among these methods, fuzzy clustering and its variants are powerful methods that have been used in MRI segmentation in which pixels are partially segmented into various tissue classes using different memberships for each tissue type. Moreover, the membership defined uniquely in a fuzzy clustering method describes the similarity between a sample and one category, which is appropriate for complex images without deterministic classification standards. Also, inherent features of brain tissues, such as overlap and closeness of tissues to each other in terms of gray-level make the classification between each category fuzzy, which complements the soft segmentation method of fuzzy clustering. This paper focuses on the FCM-based algorithm. The traditional FCM (Fuzzy c-means) algorithm only classifies in gray scale without considering the spatial information of images, obtaining good segmentation results in none-noise images. When the image is noisy and the intensity is non-homogeneous, the accuracy and robustness of the traditional FCM algorithm decline drastically. Researchers have proposed

various improved FCM algorithms to cope with the defects in MRI brain tissue segmentation. In order to overcome the limitation of FCM, Ahmed et al. [10] incorporated spatial neighborhood information into FCM algorithm with the Euclidean distance of each pixel in the neighborhood to the current pixel as a regularization. Moreover, Chen and Zhang proposed FCM_S1 and FCM_S2 [11], which simplified the neighborhood regularization of FCM_S by a mean-filter or median-filter to reduce the computational complexity.

Although a variety of image segmentation algorithms have been proposed, spatial information are not often comprehensively considered. In this paper, we incorporated the local neighborhood membership into the traditional objective function of fuzzy c-means (named FCM_anm). To reduce the negative effect of noise and lack of intensity homogeneity, a local spatial similarity measure model is established. With the measure, a local membership filtering is designed to correct the pixel membership in each iteration. Finally, we propose a novel objective function with further consideration of neighborhood membership information to improve its performance under noisy conditions. In addition, the regularization parameter in the objective function can be adaptively set according to the neighborhood information without being chosen manually. The proposed method mainly solves two challenging issues: 1) how to effectively integrate the neighborhood information and 2) how to adaptively select appropriate regularization. The consideration of membership of local neighborhood guides our model to achieve better segmentation permanence. Fig. 1 provides a visual comparison of our method and other state-of-the-arts. With the above considerations, our method achieves the best segmentation results which are much close to the ground truth in various challenging scenarios.

The rest of the paper is organized as follows. In Section 2 the conventional FCM algorithm is presented. Our proposed algorithm is explained in Section 3. Experimental and comparison results are given in Section 4 and the paper is concluded in Section 5.

II. The Fuzzy C-Means Algorithm

The FCM algorithm is a clustering algorithm based on fuzzy division, which maximizes the similarity of objects grouped into the same category and minimizes the similarity of objects between different categories. Compared with the hard classification process such as the K-means algorithm, FCM gives each object a soft fuzzy classification. The membership measures the degree of each object belonging to each category and the objects are finally divided into the category with the maximum value of membership. The objective function is as:

$$J = \sum_{i=1}^{N} \sum_{j=1}^{C} \mu_{ij}^{m} \|x_i - c_j\|^2 \tag{1}$$

$$\sum_{j=1}^{c} \mu_{ij} = 1, \forall i \tag{2}$$

where x_i is the gray value of the ith pixel, $i \in [1, N]$, N represents the scale of the image, c_j represents the prototype value of the jth cluster, $j \in [1, C]$, C is the number of clusters, μ_{ij} represents the fuzzy membership of the ith pixel with respect to cluster j. The parameter m is a weighting exponent on each fuzzy membership that determines the amount of fuzziness of the resulting classification. Applying Lagrange multipliers technique can obtain μ_{ij} and c_j.

$$\mu_{ij} = \frac{1}{\frac{\left(\|x_i - c_j\|^2\right)^{\frac{1}{m-1}}}{\sum_{k=1}^{C} \left(\|x_i - c_k\|^2\right)^{\frac{1}{m-1}}}} \tag{3}$$

$$c_j = \frac{\sum_{i=1}^{N} \mu_{ij}^{m} x_i}{\sum_{i=1}^{N} \mu_{ij}^{m}} \tag{4}$$

The process of FCM is:
Step 1 Initialize the membership and other parameters.
Step 2 Calculate c_j by (4).
Step 3 Update μ_{ij} by (3).
Step 4 If $\|\mu_{\text{old}} - \mu_{\text{new}}\| < \varepsilon$, stop. Otherwise, repeat from step 2 to step 3.

When the images are noise-free and with intensity homogeneity, the FCM algorithm shows excellent performance. However, the MRI brain images are always noisy and with intensity non-uniformity, which will result in the segmentation accuracy dropping sharply. The algorithm calculates the classification according to the isolated pixels without considering the spatial information. In contrast, the category of each pixel in every tissue is not only determined by gray level, but also related to its position in the brain. Therefore, our approach involves spatial information in the iterative process and exploits the membership filtering method to reduce the harmful effect of these drawbacks. An adaptive neighborhood penalty term without setting parameters is involved and the classification of the neighborhood around the pixel is integrated to improve robustness and make the segmentation process more efficient and accurate.

III. Proposed Method

A. Local Membership Filtering Process

To make full use of the spatial information and reduce the negative effect of noise, we design a calculation approach of distance to measure the similarity between one center pixel and its neighborhood and involve a membership filtering process using the defined similarity. The similarity with distance is defined as:

$$S\_d_{ip} = 1 - \frac{|x_i - x_p|}{\sum_{p \in N_i} |x_i - x_p|} \tag{5}$$

where x_p represents the pth pixel in the n*n neighborhood of x_i.

We also define a set $N_i^{(k)}$ composed with the membership of pixels belonging to the current category k and combine it with the new similarity to update the membership of center
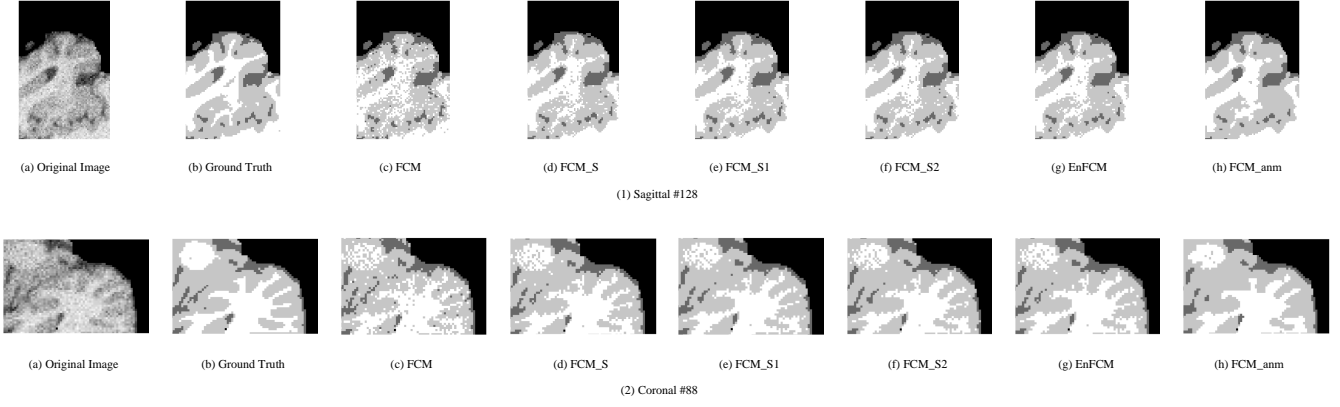
Fig. 1. A representative experimental result with partial amplification on simulated MRI brain image in coronal planes with 9% noise and 20% intensity non-uniformity: (a) Original image (b) Ground truth (c) FCM (d) FCM_S (e) FCM_S1 (f) FCM_S2. (g) EnFCM (h) FCM_anm (Our Method).

pixel i. Naturally, to ensure that the membership meets the constraint in (2), the process is defined as:

$$\mu_{ij} = \frac{\left(\frac{1}{2}\sum_{p^{(j)} \in N_i^{(j)}} S\_d_{ip}^{(j)} \mu_{pj}\right) + \mu_{ij}}{\sum_{k=1}^{C}\left(\frac{1}{2}\sum_{p^{(k)} \in N_i^{(k)}} S\_d_{ip}^{(k)} \mu_{pk}\right) + \mu_{ik}} \quad (6)$$

The process is illustrated in Fig. 2. In Fig. 2 (a), the center pixel is noise with an extreme difference in neighborhood and the pixels will be divide into two classes c_1 and c_2. After updating by (6), the center pixel membership increases from 0.13 to 0.66 for c_1 and decreases from 0.87 to 0.34 in c_2 as shown in Fig. 2 (c) and (d). Naturally, in Fig. 2 (e) the noise pixels are in the neighborhood and have significant difference with the neighbor pixels. When updating the membership of center pixel i, the membership of center pixel increases from 0.79 to 0.83 in c_1 and decrease from 0.21 to 0.17 as shown in Fig. 2 (g) and (h). It can be seen that no matter where the noise pixels appear, incorporation of the spatial neighborhood information can correct the classification result of the center pixel and reduce the negative influence of noise.

B. Objective Function in FCM_anm

Research has proven that spatial information is beneficial to FCM-based algorithms in noisy and intensity non-uniformity images. However some algorithms like FCM_S require parameters that are manually provided. Although [10] pointed out that lower SNR (signal-to-noise ratio) requires a higher value of the parameter α and a lower value of the parameter α in contrast, an improper α may lead to the loss of image information. Therefore, we design a new objective function without setting manual parameters as:

$$J = \sum_{i=1}^{N}\sum_{j=1}^{C}\mu_{ij}^{m}\|x_i - c_j\|^2 + \sum_{i=1}^{N}\sum_{j=1}^{C}\mu_{ij}^{m}L\|x_p - c_j\|^2 \quad (7)$$

$$L = \frac{1}{2N_p}\sum_{p \in N_i} S\_d_{ip}\sum_{h=1,h\neq j}^{C}\mu_{ph}^{m} \quad (8)$$
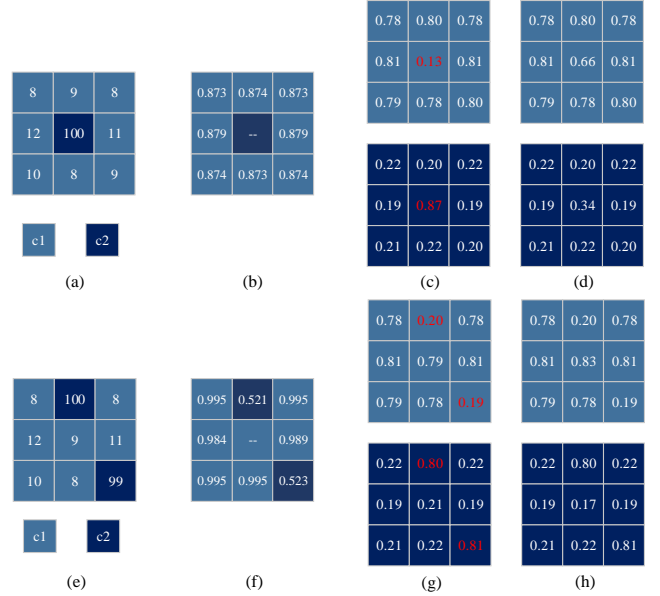

Fig. 2. The membership filtering process: (a) the center pixel is noise. (e) noise pixels are in the neighborhood. c_1 and c_2 are two categories. (b) and (f) are the S_d values of (a) and (e) according to (5). (c) and (g) are the membership before correction and (d) and (h) show the membership after correction according to (6).

Also, the constraints of the objective function is (2).

Using the Lagrange multipliers, we construct the objective function as:

$$J' = \sum_{i=1}^{N}\sum_{j=1}^{C}\mu_{ij}^{m}\|x_i - c_j\|^2 + \sum_{i=1}^{N}\sum_{j=1}^{C}\mu_{ij}^{m}L\|x_p - c_j\|^2$$
$$+\lambda_1\left(\sum_{j=1}^{C}\mu_{1j} - 1\right) + \cdots + \lambda_i\left(\sum_{j=1}^{C}\mu_{ij} - 1\right) + \cdots$$
$$+\lambda_n\left(\sum_{j=1}^{c}\mu_{nj} - 1\right)$$
$$(9)$$

To minimize the objective function, we take the derivative of J' with respect to μ_{ij} and c_{ij} respectively. Setting the

derivative equals to zero as follows:

$$\frac{\partial J'}{\partial \mu_{ij}} = m\mu_{ij}^{m-1} \left(\|x_i - c_j\|^2 + L\|x_p - c_j\|^2 \right) + \lambda_i = 0 \tag{10}$$

$$\frac{\partial J'}{\partial c_j} = \sum_{i=1}^{N} -2\mu_{ij}^m \left(x_i - c_j \right) + \sum_{i=1}^{N} -2\mu_{ij}^m L \left(x_p - c_j \right) = 0 \tag{11}$$

Substituting μ_{ij} to constrain in (2), we get:

$$1 = \sum_{j=1}^{C} \mu_{ij} = \sum_{j=1}^{C} \frac{\left(-\frac{\lambda_i}{m} \right)^{\frac{1}{m-1}}}{\left(\|x_i - c_j\|^2 + L\|x_p - c_j\|^2 \right)^{\frac{1}{m-1}}} \tag{12}$$

Then, we obtain the μ_{ij} and c_{ij} from (10) to (12) as:

$$\mu_{ij} = \frac{\left(\|x_i - c_j\|^2 + L\|x_p - c_j\|^2 \right)^{-\frac{1}{m-1}}}{\sum_{k=1}^{C} \left(\|x_i - c_k\|^2 + L\|x_p - c_k\|^2 \right)^{-\frac{1}{m-1}}} \tag{13}$$

$$c_j = \frac{\sum_{i=1}^{N} \left(\mu_{ij}^m x_i + \frac{1}{N_p} \sum_{p \in N_i} \mu_{pj}^m x_p \right)}{\sum_{i=1}^{N} \left(\mu_{ij}^m + \frac{1}{N_p} \sum_{p \in N_i} \mu_{pj}^m \right)} \tag{14}$$

The contributions of the objective function are summarized in three aspects:

- The objective function considers the relationship between each pixel and its neighborhood. If the neighboring pixels are close to the current cluster center and their memberships of other categories are relatively small, thus the membership of the center pixel in the current category increases.
- Furthermore, from (13) and (14), when x_p is noise, a smaller S_d_{ip} has a minor impact on μ_{ij} and c_j, which reduces the harmful influence of noise and facilitates a more accurate and smooth segmentation result.
- Assigning a proper value to the regularization parameter is essential and also challenging. It is unreasonable to utilize the same value of the regularization parameter for all the pixel neighborhoods while performing the segmentation or clustering. Our objective function can adaptively obtain the value of the regularization parameter without setting parameters empirically, which can avoid the loss of image information and the manual setting.

The proposed algorithm is implemented as the **Algorithm 1**.

IV. EXPERIMENTAL RESULTS

The evaluation of the proposed method is carried out on artificially synthesized images, simulated and real brain MRI images to assess its performance from both qualitative and quantitative perspectives. The simulated MRI brain datasets are provided by Brainweb [13] [14] [15] [16], which are reduction period (TR) 18 ms, reverberation period (TE) 10 ms, piece thickness 1 mm and T1-weighted. On the other hand,

---

Algorithm 1 FCM_anm

Input: $C = 3$, $m = 2$, assign ε to a small positive constant.
Output: The segmentation result.
1: Initialize $center = [c_1, c_2, c_3]$
2: **for** $i = 0$ to N **do**
3:    **for** $p = 1$ to N_p **do**
4:       calculate S_d_{ip} using (5)
5:    **end for**
6: **end for**
7: **while** $\|center_{\text{old}} - center_{\text{new}}\| < \varepsilon$ **do**
8:    **for** $i = 0$ to N **do**
9:       **for** $j = 1$ to C **do**
10:          calculate current membership using (13)
11:          **for** $p = 1$ to N_p **do**
12:             **if** $argmax(\mu_{pj}) == j$ **then**
13:                update the set $N_i^{(j)}$
14:             **end if**
15:          **end for**
16:          modify the membership using (6)
17:       **end for**
18:    **end for**
19:    update cluster centers using (14)
20: **end while**

---

the real brain MRI images were downloaded from IBSR [17]. Moreover, the proposed method is compared with previously released FCM-based algorithm which are FCM_S, FCM_S1, FCM_S2 [11] and EnFCM [18]. Dice similarity coefficient [19], Segmentation accuracy (SA) [20], Partition Coefficient (Pc) [21] and Partition Entropy (Pe) [21] are used to evaluate segmentation results. These metrics are calculated as follow:

$$Dice = \frac{2 * |A \cap G|}{|A| + |G|} \tag{15}$$

where A is the set of pixels segmented by the automatic algorithm and G is the ground truth. $Dice$ is ranged in [0,1] and the closer to 1, the better the segmentation result.

$$SA = \frac{|A \cap G|}{|G|} \tag{16}$$

SA is ranged in [0,1] and the best value is 1.

$$Pc = \frac{\sum_{i=1}^{N} \sum_{i=1}^{C} \mu_{ij}^m}{N} \tag{17}$$

Pc is ranged in (0,1) and it suggests a better segmentation result if the value is closer to 1.

$$Pe = -\frac{\sum_{i=1}^{N} \sum_{i=1}^{C} \left(\mu_{ij} \log \mu_{ij} \right)}{N} \tag{18}$$

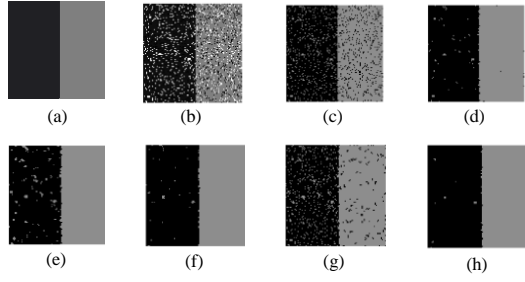Pe is ranged in (0,1) and it suggests a better the segmentation result if the value is closer to 0.

Fig. 3. Segmentation results on a synthesized image: (a) Original image (b) Image degraded with 20% salt & pepper noise (c) FCM (d) FCM_S (e) FCM_S1 (f) FCM_S2 (g) EnFCM (h) FCM_anm (Our Method).

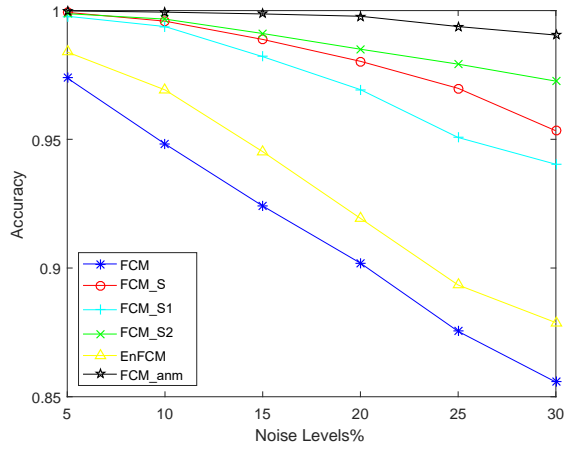Fig. 4. The accuracy of FCM, FCM_S, FCM_S1, FCM_S2, EnFCM and FCM_anm (Our Method) in different noise levels.

Fig. 5. The convergence process of our algorithm.

Fig. 6. The iteration times statistical results of FCM, FCM_S, FCM_S1, FCM_S2, EnFCM and FCM_anm (Our Method).

A. Synthesized Data

In this section, we investigate the performance of our proposed method on synthesized images. Fig. 3 shows the segmentation results of the compared algorithms. Fig. 3 (a) shows the original synthesized image which has two different classes and the salt & pepper noise is utilized to degrade the image by 20% as presented in Fig. 3 (b). Fig. 3 (c)-(h) show the segmentation results of our FCM_anm (h) with the contenders FCM, FCM_S, FCM_S1 and FCM_S2.

Obviously, the visible results prove that our method obtains better segmentation performance in noisy images. In addition, the result of our method is more stable when the noise-level increases. To better verify the robustness of the proposed method, we compare these algorithms with different noise levels in Fig. 4.

B. Simulated MRI brain images

In this section, the proposed method and the contender algorithms are evaluated on simulated MRI brain images provided by Brainwed widely used datasets. Brainweb provides a series of simulated MRI brain images with a variety of slice thickness, noise levels and levels of intensity non-uniformity. We download the T1-weighted phantom data with a slice
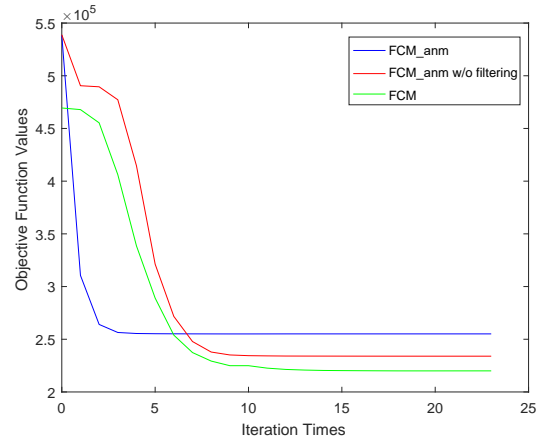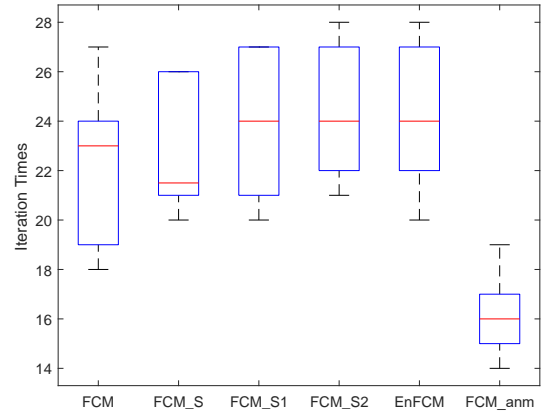
thickness of 1mm to verify the effectiveness and robustness of our algorithm. All the images contain an amount of CSF, GM and WM.

Fig. 5 illustrates how our algorithm can converge to the optimal segmentation result and the filtering process is extremely beneficial to improve the convergence speed. Moreover, our method completes the fuzzy clustering process with a fewer iterations compared with the other algorithms as the statistical results shown in Fig. 6.

Table I shows the Dice values of these competing algorithms for several brain slices in the coronal, sagittal, and transverse planes with different noise levels and 20% intensity non-uniformity levels. The results show that our method achieves a better segmentation accuracy in all the coronal, sagittal, and transverse planes. Moreover, when the noise level increases, the proposed method still maintains a good Dice value proving the robustness of our algorithm on the images with the noise effect.

Table II shows the SA values of these competing algorithms for brain slice Coronal #50 with different noise levels and intensity non-uniformity levels. When the image contains a

TABLE I
DICE OF THESE ALGORITHMS ON BRAIN SLICES CORONAL #50, TRANSVERSE #90 AND SAGITTAL #85 WITH DIFFERENT NOISE LEVELS.

		Tissue	FCM	FCM_S	FCM_S1	FCM_S2	EnFCM	FCM_anm
Coronal #50	7% noise	CSF	0.8998	0.9145	0.9153	0.9156	0.9084	0.9137
		GM	0.8909	0.9120	0.9134	0.9157	0.9115	0.9178
		WM	0.9015	0.9208	0.9229	0.9243	0.9224	0.9280
		Mean	0.8974	0.9158	0.9172	0.9185	0.9141	**0.9198**
	9% noise	CSF	0.8504	0.8940	0.8933	0.8935	0.8948	0.8929
		GM	0.8421	0.8890	0.8936	0.8937	0.8943	0.9054
		WM	0.8587	0.9003	0.9065	0.9063	0.9065	0.9179
		Mean	0.8504	0.8944	0.8978	0.8978	0.8978	**0.9054**
Transverse #90	7% noise	CSF	0.9317	0.9429	0.9407	0.9415	0.9409	0.9367
		GM	0.8769	0.9141	0.9168	0.9182	0.9080	0.9207
		WM	0.9305	0.9558	0.9584	0.9589	0.9507	0.9617
		Mean	0.9130	0.9376	0.9386	0.9395	0.9332	**0.9397**
	9% noise	CSF	0.9089	0.9319	0.9294	0.9319	0.9305	0.9280
		GM	0.8230	0.8876	0.8915	0.8931	0.8860	0.8968
		WM	0.8912	0.9393	0.9428	0.9427	0.9373	0.9444
		Mean	0.8744	0.9196	0.9212	0.9226	0.9179	**0.9316**
Sagittal #85	7% noise	CSF	0.9168	0.9307	0.9301	0.9256	0.9264	0.9208
		GM	0.8916	0.9172	0.9185	0.9215	0.9138	0.9230
		WM	0.9127	0.9369	0.9383	0.9415	0.9341	0.9465
		Mean	0.9070	0.9282	0.9290	0.9295	0.9248	**0.9301**
	9% noise	CSF	0.8890	0.9213	0.9191	0.9227	0.9163	0.9223
		GM	0.8497	0.8989	0.9047	0.9073	0.8998	0.9167
		WM	0.8842	0.9221	0.9285	0.9296	0.9237	0.9397
		Mean	0.8743	0.9141	0.9174	0.9199	0.9133	**0.9263**

TABLE II
SA OF THESE ALGORITHMS ON BRAIN SLICE CORONAL #50 WITH DIFFERENT NOISE LEVELS AND INTENSITY NON-UNIFORMITY LEVELS.

|		Tissue	FCM	FCM_S	FCM_S1	FCM_S2	EnFCM	FCM_anm
7% noise	20% INU	CSF	0.9297	0.9075	0.9306	0.9179	0.9100	0.8982
		GM	0.8615	0.8887	0.8871	0.8953	0.8876	0.9079
		WM	0.9298	0.9546	0.9536	0.9509	0.9541	0.9498
		Mean	0.8962	0.9157	0.9173	0.9190	0.9153	**0.9220**
	40% INU	CSF	0.9238	0.8273	0.9159	0.9159	0.8952	0.8863
		GM	0.8039	0.8189	0.8273	0.8351	0.8316	0.8463
		WM	0.9039	0.9270	0.9279	0.9289	0.9318	0.9371
		Mean	0.8575	0.8780	0.8768	0.8809	0.8774	**0.8855**
9% noise	20% INU	CSF	0.9129	0.9001	0.9183	0.9149	0.9056	0.8834
		GM	0.8157	0.8630	0.8668	0.8682	0.8687	0.9079
		WM	0.8707	0.9329	0.9331	0.9328	0.9366	0.9498
		Mean	0.8495	0.8940	0.8984	0.8985	0.8990	**0.9084**
	40% INU	CSF	0.9197	0.9026	0.9223	0.9153	0.9011	0.8756
		GM	0.7694	0.8160	0.8075	0.8161	0.8159	0.8463
		WM	0.8549	0.9082	0.9042	0.9054	0.9087	0.9285
		Mean	0.8216	0.8621	0.8592	0.8629	0.8620	**0.8745**
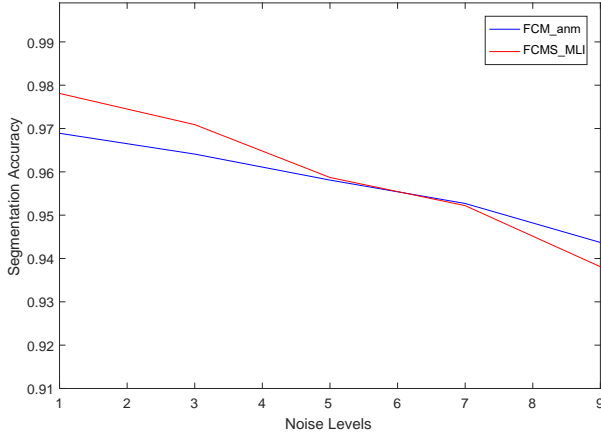
Fig. 7. Comparison with FCMS_MIL in different noise levels

TABLE III
COMPARISON WITH THE STATE-OF-THE-ART METHODS IN DIFFERENT
NOISE LEVELS AND INTENSITY NON-UNIFORMITY LEVELS.

7%noise 20%INU	C-FAFCM	0.9101
	FCM_anm	**0.9318**
7%noise 40%INU	C-FAFCM	0.9091
	FCM_anm	**0.9200**
9%noise 40%INU	FCMS-MLI	0.9044
	FCM_anm	**0.9051**

higher level of noise and intensity non-uniformity, the performance of our method is much better than the others in terms of SA due to the advantage of the context aware spatial information. Therefore, our method ensures more pixels are effectively categorized into the correct class in different levels of noise and intensity non-uniformity. The same conclusion can be found in Fig. 7, which shows the performance of FCMS_MIL [22] and our FCM_anm when varying the noise levels.

We also compare our method with C-FAFCM [23] in transverse planes slice 130 as Table III in [23] and with FCMS-MLI in transverse planes slices 35-135 as Table IX in [22]. The comparison results shown in Table III suggest that our method has better performance.

For a better visual comparison, Fig. 8 intuitively shows the segmentation results of these algorithms in coronal, sagittal and transverse planes respectively with 9% noise levels and 20% intensity non-uniformity levels.

C. Real MRI Brain Images

The competing algorithms are investigated on a set of twenty real MRI brain images provided by IBSR and the performance of these algorithms are evaluated through Pc and Pe shown in Table IV. From Table IV, the Pc of our method is much closer to 1 and Pe is closer to 0, which suggests that our algorithm has better performance when dealing with real MRI brain images. Experimental results demonstrate

that our method exhibits improvement in the segmentation performance.

V. CONCLUSION

In this paper, we proposed an accurate and robust unsupervised segmentation approach of brain MRI tissues with a fuzzy c-means based algorithm. The proposed method takes advantage of a new way in exploiting spatial information adaptively correcting the category of the center pixel by the intensity and membership of the neighborhood pixels around it to modify the fuzzy c-means objective function and to some extent preserves more image details avoiding the loss of critical information resulted in improper parameter setting. Moreover, we design the membership filtering process to correct the membership of each pixel according to the difference around its neighborhood in each iteration, which also ameliorates the segmentation result influenced maliciously by noise and intensity non-uniformity. The experimental analysis substantiates that the proposed method is appropriate for the segmentation of MRI brain images with noise and intensity non-uniformity.

REFERENCES

[1] Banerjee, Abhirup , and P. Maji . "Rough-probabilistic clustering and hidden Markov random field model for segmentation of HEp-2 cell and brain MR images." Applied Soft Computing (2016):558-576.
[2] Ur Rehman, Zaka , et al. "Fully Automated Multi-parametric Brain Tumour Segmentation using Superpixel based Classification." Expert Systems with Applications (2018).
[3] Bai, Xiangzhi , et al. "Intuitionistic Center-Free FCM Clustering for MR Brain Image Segmentation." IEEE Journal of Biomedical and Health Informatics (2018):1-1.
[4] "Atlas-based segmentation of developing tissues in the human brain with quantitative validation in young fetuses. " Human Brain Mapping 31.9(2010):1348-1358.
[5] Prastawa, Marcel , et al. "Automatic segmentation of MR images of the developing newborn brain. " Medical Image Analysis 9.5(2005):457-466.
[6] Alruwaili, Madallah , M. H. Siddiqi , and M. A. Javed . "A robust clustering algorithm using spatial fuzzy C-means for brain MR images." Egyptian Informatics Journal 21.1(2019).
[7] Chen, Yunjie , et al. "An improved anisotropic hierarchical fuzzy c-means method based on multivariate student t-distribution for brain MRI segmentation." Pattern Recognition 60(2016):778-792.
[8] Chen, Long , C. L. P. Chen , and M. Lu . "A Multiple-Kernel Fuzzy C-Means Algorithm for Image Segmentation." IEEE Trans Syst Man Cybern B Cybern 41.5(2011):1263-1274.
[9] Akkus, Zeynettin , et al. "Deep Learning for Brain MRI Segmentation: State of the Art and Future Directions." Journal of Digital Imaging (2017).
[10] Ahmed, M. N. , et al. "A modified fuzzy C-means algorithm for bias field estimation and segmentation of MRI data. " IEEE Transactions on Medical Imaging 21.3(2002):193-199.
[11] Chen, Sc , and D. Zhang . "Robust image segmentation using FCM with spatial constraints based on new kernel-induced distance measure." IEEE Transactions on Systems Man & Cybernetics Part B Cybernetics A Publication of the IEEE Systems Man & Cybernetics Society 34.4(2004):1907.

(a) #48   (b) Ground Truth   (c) FCM   (d) FCM_S   (e) FCM_S1   (f) FCM_S2   (g) EnFCM   (g) FCM_anm

(1) Sagittal planes

(a) #64   (b) Ground Truth   (c) FCM   (d) FCM_S   (e) FCM_S1   (f) FCM_S2   (g) EnFCM   (g) FCM_anm

(2) Coronal planes

(a) #106   (b) Ground Truth   (c) FCM   (d) FCM_S   (e) FCM_S1   (f) FCM_S2   (g) EnFCM   (g) FCM_anm
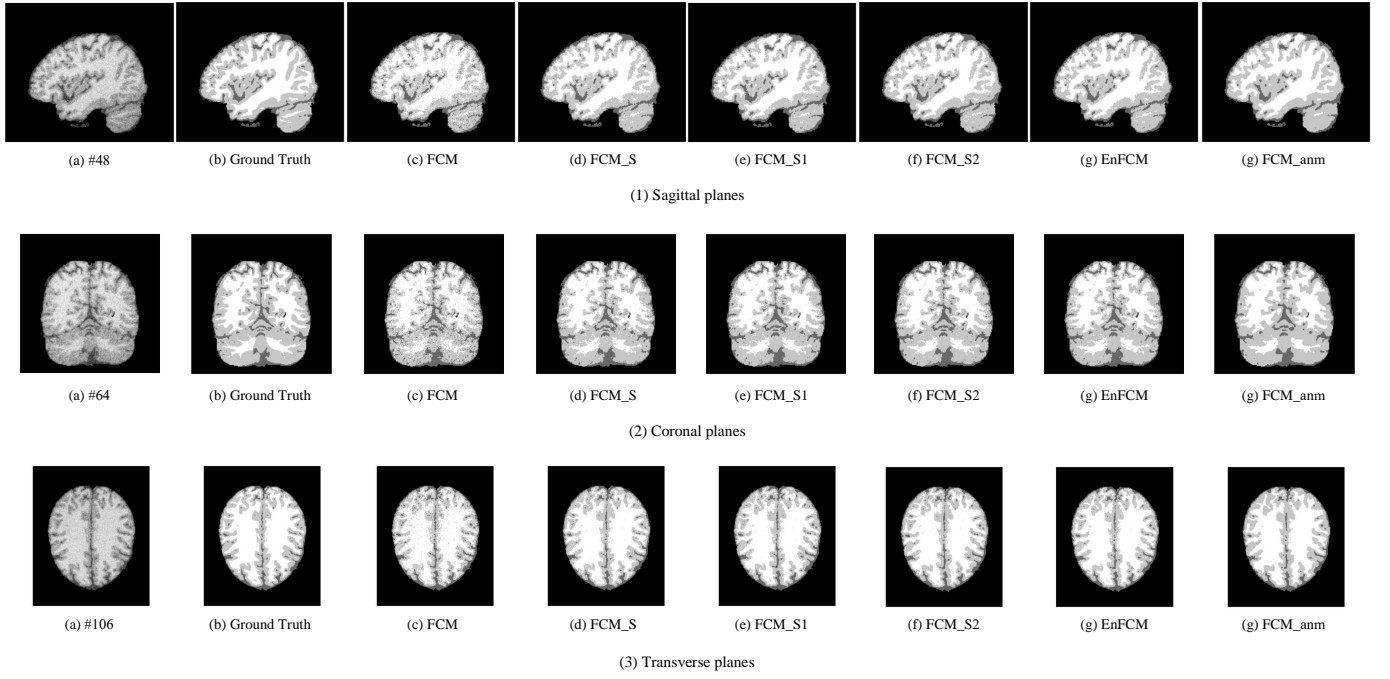
(3) Transverse planes

Fig. 8. Visible segmentation results on simulated MRI brain image with 9% noise and 20% intensity non-uniformity: (a) Original Image (b) Ground Truth (c) FCM (d) FCM_S (e) FCM_S1 (f) FCM_S2 (g) EnFCM (h) FCM_anm.

TABLE IV
Pc AND Pe (MEAN±STANDARD DEVIATION) OF COMPARABLE ALGORITHMS ON THE REAL MRI BRAIN IMAGES.

	FCM	FCM_S	FCM_S1	FCM_S2	EnFCM	FCM_anm
Mean Pc	0.8040±0.0129	0.7681±0.0095	0.7981±0.0111	0.8020±0.0129	0.7875±0.0097	**0.8343±0.0157**
Mean Pe	0.1165±0.0076	0.1366±0.0056	0.1195±0.0068	0.1177±0.0076	0.1257±0.0056	**0.1046±0.0101**

[12] Cai, Weiling , S. Chen , and D. Zhang . "Fast and robust fuzzy c-means clustering algorithms incorporating local information for image segmentation." Pattern Recognition 40.3(2007):825-838.

[13] C.A. Cocosco, V. Kollokian, R.K.-S. Kwan, A.C. Evans : "BrainWeb: Online Interface to a 3D MRI Simulated Brain Database" NeuroImage, vol.5, no.4, part 2/4, S425, 1997 – Proceedings of 3-rd International Conference on Functional Mapping of the Human Brain, Copenhagen, May 1997.

[14] R.K.-S. Kwan, A.C. Evans, G.B. Pike : "MRI simulation-based evaluation of image-processing and classification methods" IEEE Transactions on Medical Imaging. 18(11):1085-97, Nov 1999.

[15] R.K.-S. Kwan, A.C. Evans, G.B. Pike : "An Extensible MRI Simulator for Post-Processing Evaluation" Visualization in Biomedical Computing (VBC'96). Lecture Notes in Computer Science, vol. 1131. Springer-Verlag, 1996. 135-140.

[16] D.L. Collins, A.P. Zijdenbos, V. Kollokian, J.G. Sled, N.J. Kabani, C.J. Holmes, A.C. Evans : "Design and Construction of a Realistic Digital Brain Phantom" IEEE Transactions on Medical Imaging, vol.17, No.3, p.463–468, June 1998.

[17] NITRC. (2016). The Internet Brain Segmentation Repository. [Online].Available: https://www.nitrc.org/projects/ibsr/

[18] Szilagyi, L. , et al. "MR brain image segmentation using an enhanced fuzzy C-means algorithm." International Conference of the IEEE Engineering in Medicine & Biology Society IEEE, 2003.

[19] Dice, Lee R. "Measures of the Amount of Ecologic Association Between Species." Ecology 26.3(1945).

[20] "Conditional spatial fuzzy C-means clustering algorithm for segmentation of MRI images." Applied Soft Computing 34(2015):758-769.

[21] Qiu, Cunyong , et al. "A modified interval type-2 fuzzy C-means algo-rithm with application in MR image segmentation." Pattern Recognition Letters 34.12(2013):1329-1338.

[22] Kouhi, Abolfazl , H. Seyedarabi , and A. Aghagolzadeh . "Robust FCM clustering algorithm with combined spatial constraint and membership matrix local information for brain MRI segmentation." Expert Systems with Applications 146(2019):113159.

[23] Ghosh, Partha , K. Mali , and S. K. Das . "Chaotic Firefly Algorithm-Based Fuzzy C-Means Algorithm for Segmentation of Brain Tissues in Magnetic Resonance Images." Journal of Visual Communication and Image Representation 54.JUL.(2018):63-79.